J Mol Model (2015) 21:40
DOI 10.1007/s00894-015-2588-2

ORIGINAL PAPER

Ordered and layered structure of liquid nitromethane within a graphene bilayer: toward stabilization of energetic materials through nanoscale confinement

Yingzhe Liu · Tao Yu · Weipeng Lai · Ying Kang · Zhongxue Ge

Received: 30 October 2014 / Accepted: 26 January 2015

Abstract The structural characteristics involving thermal stabilities of liquid nitromethane (NM)—one of the simplest energetic materials—confined within a graphene (GRA) bilayer were investigated by means of all-atom molecular dynamics simulations and density functional theory calculations. The results show that ordered and layered structures are formed at the confinement of the GRA bilayer induced by the van der Waals attractions of NM with GRA and the dipole–dipole interactions of NM, which is strongly dependent on the confinement size, i.e., the GRA bilayer distance. These unique intermolecular arrangements and preferred orientations of confined NM lead to higher stabilities than bulk NM revealed by bond dissociation energy calculations.

Keywords Encapsulation · Dipole-dipole interaction · Thermal stability · Molecular dynamics simulation · Density functional theory calculation

Introduction

Energetic materials confined into specific nanoscale spaces have attracted much attention since their stabilities at ambient pressure and room temperature can be improved to effectively balance the intrinsic contradiction between power and safety [1–6]. Due to the experimental difficulties and cost of synthesis of high energy density materials, theoretical research has played an important role in exploring their structural and electronic properties from a microscopic viewpoint, while helping design new propellants, explosives, and pyrotechnics. Recent quantum chemistry calculations suggested that graphene (GRA) sheets are good candidates for encapsulating and stabilizing various energetic materials, including polymeric nitrogen, HMX (octahydro-1,3,5,7-tetranitro-1,3,5,7-tetrazocine), FOX-7 (1,1-diamino-2,2-dinitroethylene), RDX (hexahydro-1,3,5-trinitro-striazine), etc. The stabilization mechanism is governed by charge transfer, intermolecular H-bonding, and dispersion interactions between energetic molecules and GRA sheets [7, 8]. Furthermore, functionalized GRA sheets can enhance the thermal decomposition of organic explosives [9]. The confinement between GRA sheets, therefore, potentially leads to optimal performance and controlled energy release of energetic molecules. Despite the importance of confined energetic materials, knowledge of their stabilization mechanisms, which involve intermolecular arrangements, orientations, and nature interactions, is still fragmentary.

Here, the structural characteristics associated with thermal stabilities of energetic materials through nanoscale confinement were investigated theoretically by encapsulating the simplest organic explosive nitromethane (NM) within a GRA bilayer. The effect of confinement size was also considered by regulating the GRA bilayer distance from 6 Å to 14 Å at an interval of 1 Å. The typical structural motifs of confined NM were found by molecular dynamics (MD) simulations, and the corresponding thermal stabilities were examined by bond dissociation energy (BDE) obtained from density functional theory (DFT) calculations. The results reported in this work are envisioned to provide new insights for improving the safety of energetic materials.

Y. Liu (✉) · T. Yu · W. Lai · Y. Kang · Z. Ge
Xi'an Modern Chemistry Research Institute, Xi'an 710065, People's Republic of China
e-mail: liuyz_204@163.com

T. Yu
School of Materials Science and Engineering, Fuzhou University, Fuzhou 350108, People's Republic of China

Published online: 13 February 2015

Methods

Molecular models

The initial model of NM solvent was taken from our previous work [10]. The CHARMM36 general force field [11] was used to describe the NM molecule, which reproduces the experimental density of liquid NM well. Two ideal and armchair GRA sheets were built employing the visual molecular dynamics (VMD) package [12]. The normal vector of GRA sheets was aligned along the *z*-axis, and the edge lengths along *x*- and *y*- axis were both chosen to be about 25 Å (see Fig. 1). All the GRA atoms were described by the sp^2 aromatic carbon parameters of the CHARMM27 force field [13] devoid of a net atomic charge. The position of all GRA atoms was restrained in all simulations by means of a weak harmonic potential of 1.0 kcal mol^{-1}.

Molecular dynamics simulations

All MD simulations were carried out using the program NAMD2.9 [14] using the isobaric-isothermal ensemble. Periodic boundary conditions were applied in three-dimensional (3D) Cartesian space. Covalent bonds involving hydrogen atoms were constrained to their equilibrium lengths with the aid of the SHAKE/RATTLE algorithms [15, 16]. A smoothed 12 Å spherical cutoff was chosen to truncate van der Waals forces, and long-range electrostatic interactions were evaluated using the particle mesh Ewald (PME) approach [17]. The equations of motion were integrated through the multiple time-step Verlet r-RESPA algorithm [18] with time steps of 2 and 4 fs for short- and long-range interactions, respectively. The temperature and pressure were maintained at 300 K and 1 bar by Langevin dynamics and the Langvein piston pressure control [19]. Each production simulation was carried out for 10 ns and the trajectory of the final 5 ns was analyzed. Visualization and analysis of MD trajectories were performed with the VMD package [12].

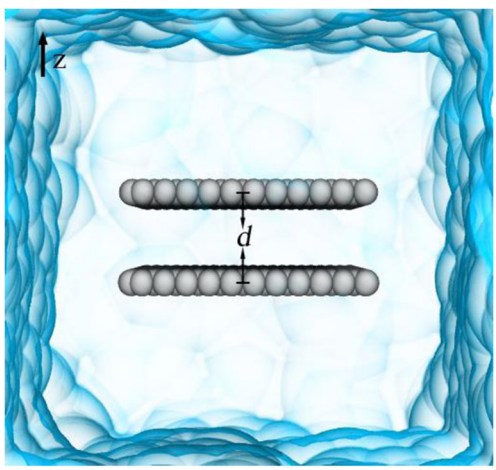

Fig. 1 Initial structure of a graphene (GRA) bilayer immersed in liquid nitromethane (NM) solvent for molecular dynamic (MD) simulations. In this study, the distance, *d*, between the two GRA sheets ranges from 6 Å to 14 Å at an interval of 1 Å

Bond dissociation energy

The BDE, E_{BD}, was calculated by the following equation:

$$E_{BD}(A{-}B) = E_{A\cdot} + E_{B\cdot} - E_{A-B} \quad (1)$$

where A–B stands for the NM molecule; A· and B· for the radicals produced from dissociation of the A–B bond; E_{A-B}, $E_{A\cdot}$, and $E_{B\cdot}$ are the corresponding electronic energies. The electronic energy was calculated at the B3LYP level [20, 21] of the DFT method with the 6-31G* basis set [22] employing the Gaussian program [23]. Here, only breaking of the C–N bond in NM was considered, which is generally deemed the most probable initiation of NM decomposition [24].

Results and discussion

The simulation trajectories show that NM molecules cannot spontaneously enter the interior of two GRA sheets at a distance of 6 Å. Hence, the simulation results for the other molecular systems are discussed in the following.

Mass density distributions

To assess the distribution induced by the confinement on NM, the mass density distribution along the normal to GRA bilayer was calculated and is depicted in Fig. 2. High mass densities and layered distributions of NM were observed between the two GRA sheets owing to the unique intermolecular arrangements. The highest density of NM was located at the center of the GRA bilayer at a distance of 7 Å. As the bilayer distance increased, the center density decreased gradually driven by the van der Waals attractions between NM molecules and GRA sheets. The single peak also became wider and tended to split into two peaks. Two peaks are fully formed and no NM molecules exist at the center of the GRA bilayer at a bilayer distance of 10 Å. For bilayer distances ranging from 11 to 13 Å, similarly, the density is lower and the corresponding distribution is less concentrated. When the bilayer distance is 14 Å, three peaks are found and the middle peak located at the center of the GRA bilayer has the highest density. From the above results, it can be deduced that the layered

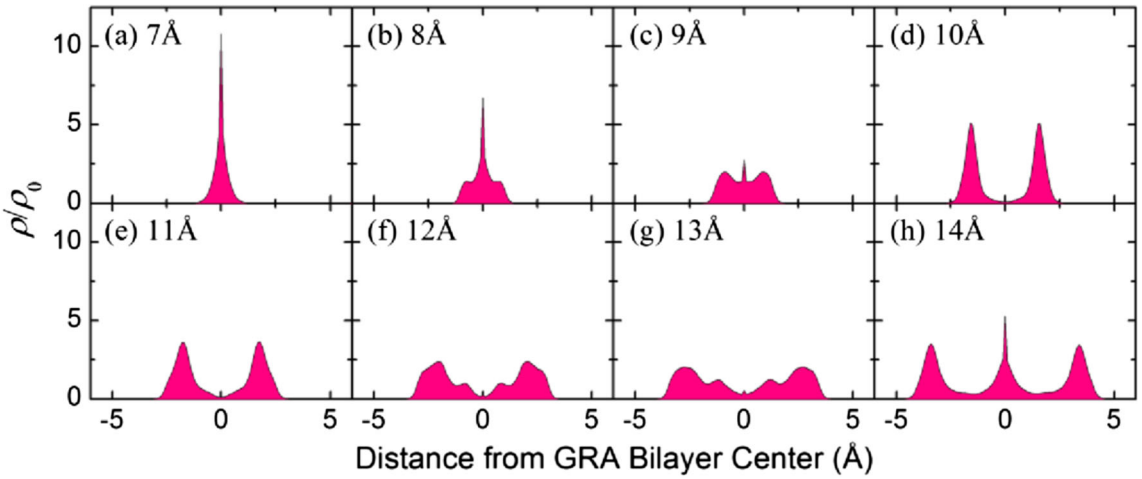

Fig. 2 Mass density profiles of confined NM determined along the normal to the GRA bilayer at a series of distances; ρ_0 is the mass density of bulk NM

distribution of confined NM is strongly dependent on the GRA bilayer distance, which is different from the distribution of pure liquid NM. Previous simulations have shown that the first neighbor shell is within a radius of about 6 Å, and the second shell is within about 11 Å for a given NM molecule [25, 26].

Dipole orientations

To understand the orientations of NM encapsulated in the GRA bilayer, the distribution of the orientation angle, θ, formed between the NM dipole and the normal to the GRA bilayer was calculated. As displayed in Fig. 3, a peak around the orientation angle of 90° appears in all systems, suggesting that the dipole of confined NM prefers to be parallel with the GRA sheets. It is expected that peak height will depend strongly on the distance to the GRA bilayer. However, the peak height does not decrease monotonously as the bilayer distance increases. For instance, the peak height for a distance of 10 Å is lower than that for a distance of 7 Å but higher than that for a distance of both 8 and 9 Å. Moreover, there is another preferred orientation when the GRA bilayer distance is 9 Å, i.e., the NM dipole is perpendicular to the GRA sheet. Hence, it can be seen that a suitable distance of GRA bilayer plays a key role in the formation of ordered and layered structures of NM with preferred orientations.

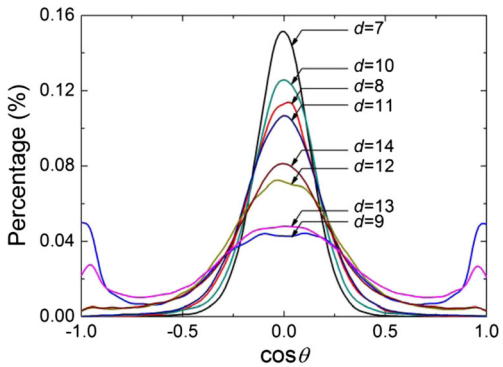

Fig. 3 Distributions of cosθ within a series of the GRA bilayer; θ is defined as the angle formed between the NM dipole and the normal to the GRA bilayer

Confined structures

The typical structural arrangements and dipole orientations of NM confined within the GRA bilayer obtained from the simulation trajectories are shown in Fig. 4. It is evident from Fig. 4a that the one-layer structure of confined NM exhibits a highly ordered arrangement, i.e., the NM dipoles were arrayed head-to-tail in a linear arrangement parallel to the GRA sheets induced by the favored dipole–dipole interactions. As the bilayer distance increased to 9 Å, a staggered arrangement of dipoles perpendicular to the GRA sheets was observed (see Fig. 4b), which can be attributed to the balance of the dipole–dipole interactions and the van der Waals attractions between NM and GRA. For the two-layer structure, a head-to-tail alignment of NM dipoles was also found, arranged in a staggered manner to avoid layer–layer repulsive interactions (see Fig. 4c). For the three-layer structure, in contrast, the arrangement of NM dipoles was less ordered and did not maintain the linear pattern. This is because the confinement effect of the GRA bilayer on NM would be gradually weakened as the distance of the GRA bilayer increases. Nevertheless, it can be seen from each separating layer structure that the NM dipoles still tend to be arranged in head-to-tail orientation as much as possible (see Fig. 4d–g).

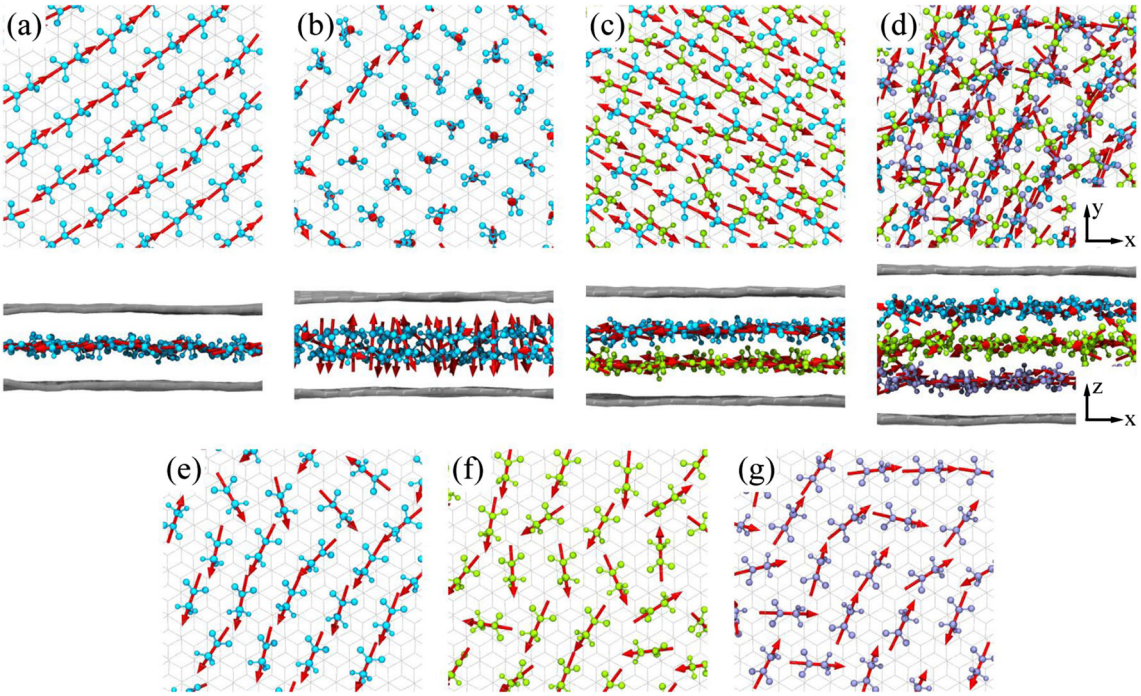

Fig. 4a–g Typical structures obtained from MD simulations of NM confined within the GRA bilayer. Distances between the two GRA sheets (Å): **a** 7, **b** 9, **c** 10, **d** 14; **e–g** correspond to the three layers of **d**, respectively. *Red arrows* NM dipoles

Thermal stabilities

As proposed by Zhang [27], the BDE of a NM dimer with different arrangements and orientations can be employed to simply estimate the stability of NM against external stimuli such as tension, compression, sliding, and rotational shear. Herein, two typical arrangement motifs were extracted to represent the NM structures within the GRA bilayer, i.e., linear and parallel NM dimers. The thermal stabilities of confined NM were evaluated by the BDE calculations of two typical arrangement motifs via scanning the possible orientations, where the NM dimers were treated as rigid.

For the linear NM dimer, the head-to-tail arrangement has the highest BDE, indicative of the most stable structure, while the C–N bond is easiest to break for head-to-head arrangement (see Fig. 5). For the parallel NM dimer, the staggered arrangement has higher stability than the eclipsed arrangement (see Fig. 6). It is evident that the most stable arrangements and orientations in two typical structural motifs can be induced by the confinement of the GRA bilayer (see Fig. 4). Compared with the disordered structure of bulk liquid NM [10], therefore, the ordered and layered structure formed within the GRA bilayer leads to higher stability.

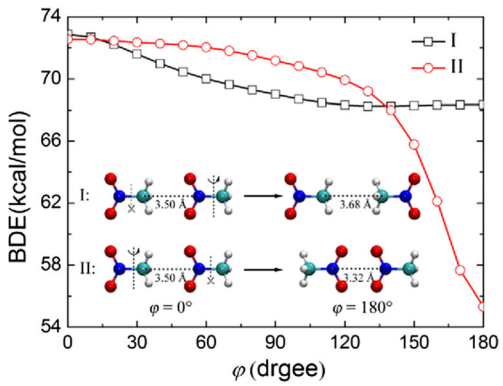

Fig. 5 Bond dissociation energy (BDE) of the linear NM dimer as a function of rotational angle with two orientations: orientation I represents the transformation from head-to-tail to tail-to-tail arrangement; orientation II represents the transformation from head-to-tail to head-to-head arrangement

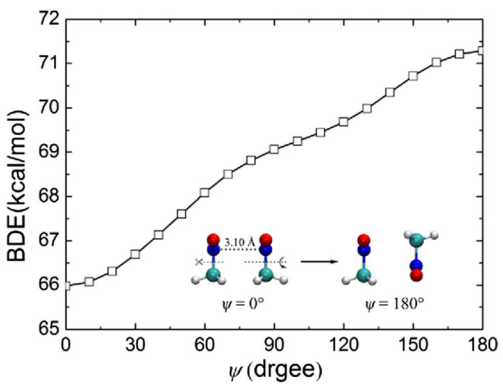

Fig. 6 BDE of the parallel NM dimer as a function of rotational angle transforming from eclipsed to staggered arrangement

Conclusions

MD simulations and DFT calculations were carried out to study the structural characteristics involving thermal stabilities of liquid NM encapsulated within a GRA bilayer. GRA bilayer confinement can induce the formation of ordered and layered structures of NM resulting from dipole–dipole interactions and van der Waals attractions between NM and GRA, which is correlated strongly to the GRA bilayer distance. The BDE calculations show that the unique intermolecular arrangements and orientations of confined NM have higher thermal stabilities than bulk NM. The results reported herein further improve our understanding of the stabilization of energetic materials through nanoscale confinement.

Acknowledgments This study was supported by the National Natural Science Foundation of China (Nos. 21403162).

References

1. Abou-Rachid H, Hu A, Timoshevskii V, Song Y, Lussier LS (2008) Phys Rev Lett 100:196401
2. Ji W, Timoshevskii V, Guo H, Abou-Rachid H, Lussier LS (2009) Appl Phys Lett 95:021904
3. Zheng FW, Yang Y, Zhang P (2012) Int J Mod Phys B 26:1250047
4. Sharma H, Garg I, Dharamvir K, Jindal VK (2010) J Phys Chem C 114:9153–9160
5. Ren XY, Liu ZY (2005) Struct Chem 16:567–570
6. Tang CM, Zhu WH, Deng KM (2009) Chin Phys Lett 26:096101
7. Timoshevskii V, Ji W, Abou-Rachid H, Lussier LS, Guo H (2009) Phys Rev B 80:115409
8. Smeu M, Zahid F, Ji W, Guo H, Jaidann M, Abou-Rachid H (2011) J Phys Chem C 115:10985–10989
9. Liu LM, Car R, Selloni A, Dabbs DM, Aksay IA, Yetter RA (2012) J Am Chem Soc 134:19011–19016
10. Liu YZ, Lai WP, Yu T, Ge ZX, Kang Y (2014) J Mol Model 20:2459
11. Vanommeslaeghe K, Hatcher E, Acharya C, Kundu S, Zhong S, Shim J, Darian E, Guvench O, Lopes P, Vorobyov I, Mackerell AD (2010) J Comput Chem 31:671–690
12. Humphrey W, Dalke A, Schulten K (1996) J Mol Graph 14:33–38
13. MacKerell AD, Bashford D, Bellott M, Dunbrack RL, Evanseck JD, Field MJ, Fischer S, Gao J, Guo H, Ha S, Joseph-McCarthy D, Kuchnir L, Kuczera K, Lau FTK, Mattos C, Michnick S, Ngo T, Nguyen DT, Prodhom B, Reiher WE, Roux B, Schlenkrich M, Smith JC, Stote R, Straub J, Watanabe M, Wiorkiewicz-Kuczera J, Yin D, Karplus M (1998) J Phys Chem B 102:3586–3616
14. Phillips JC, Braun R, Wang W, Gumbart J, Tajkhorshid E, Villa E, Chipot C, Skeel RD, Kale L, Schulten K (2005) J Comput Chem 26: 1781–1802
15. Ryckaert JP, Ciccotti G, Berendsen HJC (1977) J Comput Phys 23: 327–341
16. Andersen HC (1983) J Comput Phys 52:24–34
17. Darden T, York D, Pedersen L (1993) J Chem Phys 98:10089–10092
18. Tuckerman M, Berne BJ, Martyna GJ (1992) J Chem Phys 97:1990–2001
19. Feller SE, Zhang Y, Pastor RW, Brooks BR (1995) J Chem Phys 103: 4613–4621 9
20. Lee C, Yang W, Parr RG (1988) Phys Rev B 37:785–789
21. Becke AD (1993) J Chem Phys 98:5648–5652
22. Hariharan PC, Pople JA (1973) Theor Chim Acta 28:231–222
23. Frisch MJ, Trucks GW, Schlegel HB, Scuseria GE, Robb MA, Cheeseman JR, Scalmani G, Barone V, Mennucci B, Petersson GA, Nakatsuji H, Caricato M, Li X, Hratchian HP, Izmaylov AF, Bloino J, Zheng G, Sonnenberg JL, Hada M, Ehara M, Toyota K, Fukuda R, Hasegawa J, Ishida M, Nakajima T, Honda Y, Kitao O, Nakai H, Vreven T, Montgomery JA Jr, Peralta JE, Ogliaro F, Bearpark M, Heyd JJ, Brothers E, Kudin KN, Staroverov VN, Kobayashi R, Normand J, Raghavachari K, Rendell A, Burant JC, Iyengar SS, Tomasi J, Cossi M, Rega N, Millam JM, Klene M, Knox JE, Cross JB, Bakken V, Adamo C, Jaramillo J, Gomperts R, Stratmann RE, Yazyev O, Austin AJ, Cammi R, Pomelli C, Ochterski JW, Martin RL, Morokuma K, Zakrzewski VG, Voth GA, Salvador P, Dannenberg JJ, Dapprich S, Daniels AD, Farkas O, Foresman JB, Ortiz JV, Cioslowski J, Fox DJ (2009) Gaussian 09. Gaussian Inc, Wallingford
24. Zhang CY, Wang XL, Zhou MF (2011) J Comput Chem 32:1760–1768
25. Seminario JM, Concha MC, Politzer P (1995) J Chem Phys 102:8281
26. Howard EA, Abu-Awwad F, Politzer P (1999) J Chem Phys B 103: 9738–9742
27. Zhang CY (2013) J Mol Model 19:477–483